PROCEEDINGS OF SCIENCE

Pitch-angle distribution of TeV cosmic rays in the LISM

Ming Zhang,[a,*] **Noufel Maalal**[a] **and Nikolai Pogorelov**[b]

[a] *Department of Aerospace, Physics and Space Sciences, Florida Institute of Technology, 150 W. University Blvd., Melbourne, FL 32940, USA*

[b] *Department of Space Science and Center for Space Plasma and Aeronomic Research University of Alabama in Huntsville 301 Sparkman Drive, Huntsville, AL 35899, USA*

E-mail: mzhang@fit.edu

The electric and magnetic fields encountered by Galactic TeV cosmic rays (CRs) as they propagate deep into the heliosphere can alter their energy and arrival direction upon reaching Earth. This perturbation of trajectories in phase space can distort the angular distribution of particle flux, also known as anisotropy. The maps of TeV CR anisotropy obtained by air shower experiments appear quite complex. To remove heliospheric distrortions, we developed a theory of flux mapping based upon applying Liouville's theorem to the CR trajectories obtained via a multi-fluid magnetohydrodynamic model of the heliosphere. With this technique, we determined the original CR distribution function in the pristine local interstellar medium. In this paper, we focus on the dependence of TeV CR intensity on the particle pitch-angle relative to the direction of the local interstellar magnetic field. The pitch-angle distribution has two significant features: it is dominated by a dipole anisotropy, and it displays a notable increase in particle intensity towards the direction aligning with the magnetic field at the zero pitch angle. The dipole anisotropy suggests that TeV CRs are scattered nearly isotropically by the interstellar magnetic field turbulence instead of expected behavior resulting from resonant scattering by turbulence with a Kolmogorov power spectrum. The increase of particles towards zero pitch-angle implies particle focusing by an inhomogeneous interstellar magnetic field with a gradient length approximately equal to 6 times the CR mean free path.

38th International Cosmic Ray Conference (ICRC2023)
26 July - 3 August, 2023
Nagoya, Japan

ICRC2023
38th International Cosmic Ray Conference
The Astroparticle Physics Conference

*Speaker

PoS(ICRC2023)328

1. Introduction

Galactic cosmic rays (CRs) below the knee energy ($\sim$ 3000 TeV) are most likely accelerated by supernovae. Below this energy, charged particles are confined by the interstellar magnetic fields through gyration along the mean magnetic field, and through pitch angle scattering which prevents them from streaming away along the magnetic field lines. As a result, charged particles below the knee can spend tens of millions of years in the Galaxy before some of them reach the Earth and are detected by experiments. The speed at which CRs can propagate from their sources to reach our planet is largely affected by the properties of the magnetic field, such as its strength, inhomogeneity, motional velocity, and fluctuations or turbulence. Therefore, while measuring the CR spectrum and its composition can provide insight into CR sources and interstellar propagation, the study of the anisotropy of CR intensity as a function of arrival direction on Earth can provide more detailed understanding of CR propagation. For instance, if there is a relatively recent source located within a few particle mean free paths from us, there may exist some signature of the point source in anisotropy measurements. This prospect has motivated teams of air shower experimentalists to study CR anisotropy. So far, the observed sky maps show that the anisotropy amplitude of TeV CRs is rather small, about 10^{-4} – 10^{-3} in relative intensity [e.g. 1–3]. The anisotropy patterns appear broad and complex, puzzling many of us who are trying to reconstruct the physical mechanisms responsible for the observations.

Earth resides near the center of the heliosphere carved from the local interstellar medium (LISM) by the solar wind (SW) plasma, within which the electric and magnetic fields are drastically different from those in the LISM. The heliosphere affects the distribution of local interstellar quantities at distances exceeding 10^4 AU. The radial distance to the heliopause in all directions is larger than the gyroradius of TeV CRs in a typical interstellar magnetic field of $\sim 3\ \mu$G. The electric and fields within the heliosphere can severely alter the trajectories of these CRs on their way to Earth, changing their arrival direction and energy, and consequently distorting the patterns of CR anisotropy. Thus, in order to use the anisotropy measurements to understand the CR propagation in the interstellar medium, we must remove the effects of heliospheric distortion. We have developed a theory of applying Liouville's theorem to map the CR distribution function from the interstellar medium to Earth [18, 19]. We reconstructed from the particle distribution as a function of the particle pitch-angle relative to the local interstellar magnetic field, or the interstellar pitch-angle distribution, by removing several other contributions to the observed anisotropy. The result sheds light on to the physics of CR transport mechanisms in the LISM.

2. Method

CR flux is proportional to the particle distribution function in the observer's reference frame [18]. Due to Liouville's theorem and to Lorentz invariance, one can map the particle distribution from the interstellar space to Earth along particle trajectories in the phase space, which can calculated using the Lorentz force with a model of the heliospheric electric and magnetic fields. We used the magnetohydrodynamic (MHD) heliosphere model produced by the Multi-scale Fluid-Kinetic Simulation Suite of the University of Alabama in Huntsville [4, 9, 10]. This simulation package solves the multi-fluid MHD equations for plasmas coupled with the kinetic (or multi-fluid) transport

models for neutral atoms, and takes into account the physics of space plasma/magnetic field and neutral gas interaction. The inputs, the SW parameters, and the LISM properties were estimated as accurately as possible under the constraints set by *in-situ* observations of the SW and of solar magnetic field in the inner heliosphere over many solar cycles [15–17], and in the outer heliosphere. These were obtained respectively by many heliospheric missions and by the Voyagers and remote-sensing observations of the NASA Interstellar Boundary Explorer (IBEX) mission. In particular, with the help of the heliosphere model, it was possible to use the Voyager measurements in the LISM beyond the heliopause [12–14] to greatly constrain the interstellar magnetic field and the gas parameters, even though the spacecraft has not reached the unperturbed interstellar medium. The model has also helped greatly in interpreting IBEX observations of energetic neutral atom fluxes originating from the heliospheric boundary region [e.g., 5, 8, 20]. Moreover, the model was validated against other *in-situ* and remote observations, e.g., SOHO Lyα backscattered emission, Lyα absorption profiles in the direction of nearby stars, New Horizons observations in the distant SW [see, e.g., 6, 7]. The output of the MHD heliosphere simulation includes solutions to the distribution of magnetic field vector $\mathbf{B}$ and plasma velocity $\mathbf{V}$. Since the SW and interstellar plasmas are highly conductive, we can calculate the electric field distribution using the ideal MHD Ohm's law, i.e., $\mathbf{E} = -\mathbf{V} \times \mathbf{B}$.

The electric and magnetic fields contained in the heliosphere model are the average fields. They do not contain rapidly-varying fluctuations. The calculations of particle trajectories used to map CR flux can suffer some inaccuracy. However, because heliospheric field fluctuations typically have scales much smaller than the gyroradius of TeV CRs, the perturbations caused by the unknown fluctuating fields are negligible compared to the trajectory curvature caused by the large-scale heliospheric magnetic field. Similarly, fluctuating interstellar magnetic fields can only cause significant scattering over a time-scale of a few years, as estimated from the typical length of particle mean free paths. During propagation through the heliosphere, which typically only lasts a few days, the effect of fluctuating interstellar magnetic fields is also negligible. Therefore we can safely use the Lorentz force from the fields generated by the MHD heliosphere model to calculate CR trajectories and map CR flux.

The mapping of the CR distribution function requires us to know it either on Earth or in the LISM. Measurements on Earth make it possible to quantify the momentum dependence, but not the spatial dependence of the particle distribution. Thus, we cannot directly map out the measurements of CR fluxes to the LISM. Instead, we assume a certain form of particle distribution in the LISM, map it to Earth, and verify if the mapped distribution matches observations on Earth. Because the observed CR anisotropy is small and its energy dependence must be very close to the observed CR energy spectrum, we take a perturbation form. We expand the dependence of particle distribution function on interstellar pitch-angle cosine μ and particle guiding center location ($\mathbf{R}_g = \mathbf{r} - \boldsymbol{\rho}_g$), which is displaced by a gyroradius $\boldsymbol{\rho}_g = \frac{\mathbf{B}_{ism} \times \mathbf{p}}{q B_{ism}^2}$ of the particle with charge q and momentum $\mathbf{p}$ in interstellar magnetic field $\mathbf{B}_{ism}$.

$$f(\mathbf{r}, \mathbf{p}) = f_0 p^{-\gamma} \left[1 + \mathbf{G}_\perp \cdot \mathbf{R}_g + PAD(\mu)\right] \tag{1}$$

Here p is the magnitude of particle momentum vector, $\gamma \approx 4.75$ is the slope of the CR power-law momentum distribution, f_0 is a reference constant, $\mathbf{G}_\perp = \nabla_\perp \ln f$ is the spatial gradient of particle

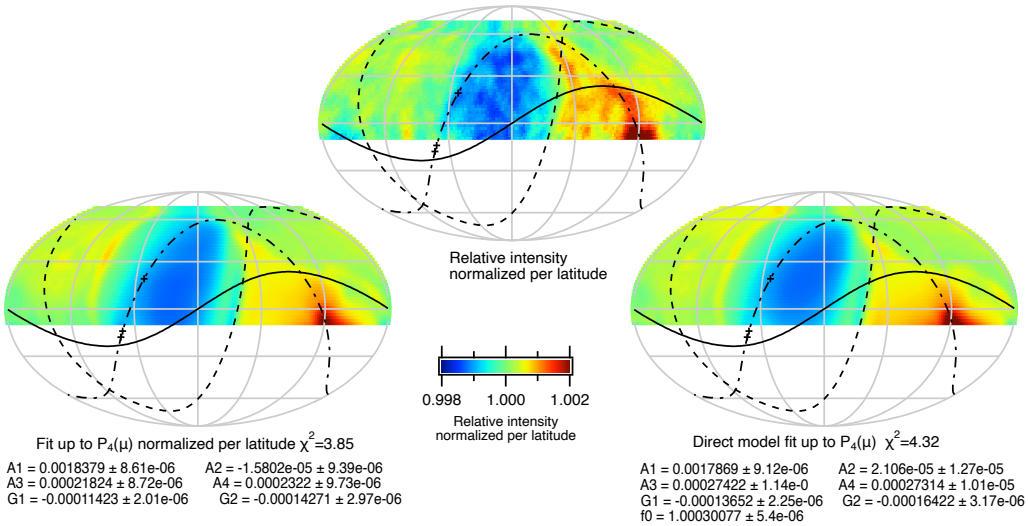

Figure 1: Anisotropy map of 4 TeV CR as measured in the Tibet Air Shower experiment (middle), the Liouville mapping model calculation with least-χ^2 linear fit (right) and nonlinear fit (left). The solid, dashed, and dash-dotted curves show the ecliptic plane, the plane perpendicular to LISM magnetic field and passing through the Sun, and the hydrogen deflection plane, respectively.

intensity perpendicular to the LISM and pitch-angle distribution $PAD(\mu)$ is the expanded into a series of Legendre polynomials up to an order of N

$$PAD(\mu) = \sum_{n=1}^{N} A_n P_n(\mu) \tag{2}$$

where the linear coefficient A_n is commonly referred to as the amplitudes of pitch-angle anisotropy of N-th order. Once the interstellar distribution in Equation (1) is mapped to Earth, we can compare its output with the observed angular map of CR anisotropy of relative intensity to determine the parameters A_n and $\mathbf{G}_\perp$.

While air shower experiments can accurately measure the arrival direction of individual CRs, they cannot determine particle flux accurately enough to distinguish minute variations of CR anisotropy at the level of 10^{-4} to 10^{-3}. The determination of flux variation in longitude (right ascension) can rely on the Earth's spin, but the sensitivity to latitudinal (declination) variation is not obtainable. Thus generally, in anisotropy measurements presented by experimental teams, the so-called relative intensity as a function of declination δ and right ascension α is defined as:

$$I(\delta,\alpha) = \frac{f(\mathbf{r}((\delta,\alpha),\mathbf{p})}{\int_0^{2\pi} f(\mathbf{r}((\delta,\alpha),\mathbf{p}) d\alpha} \tag{3}$$

We fit Equation (3) to the 4 TeV anisotropy data provided by Tibet ASγ using a nonlinear optimization procedure. The nonlinear fit has improved the reduced χ^2 value of fitting from 4.32 to 3.85, even though the degree of freedom is reduced by 1. Figure 1 shows a comparison between the fits produced by Equation (3) and (1), and the experimental skymap for comparison.

If our anisotropy model is correct, we can reconstruct the true relative intensity of interstellar

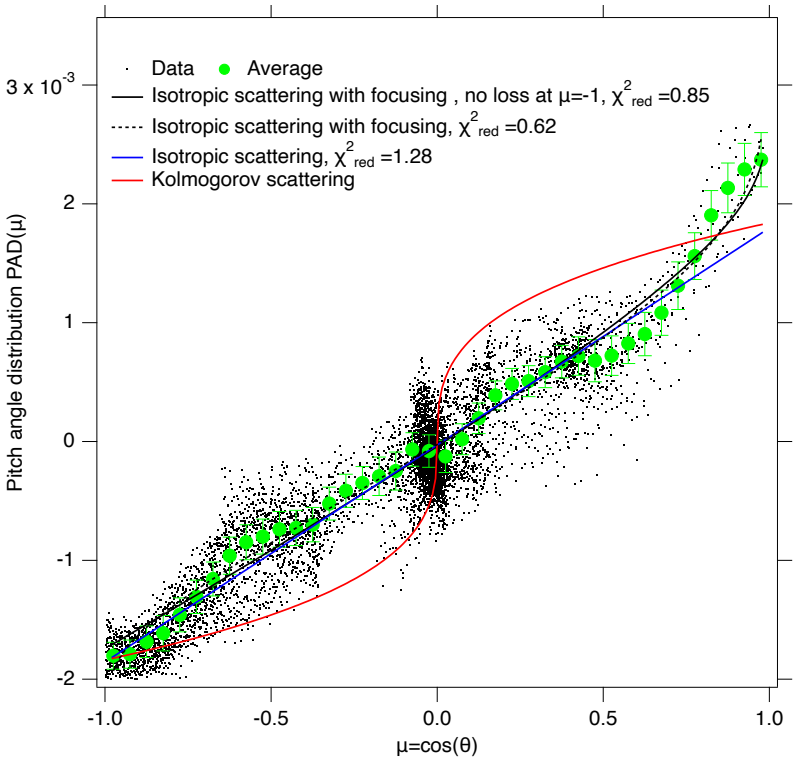

Figure 2: Relative pitch-angle distribution as a function of particle pitch-angle in the LISM after the other anisotropies are removed and the arrival direction is corrected. The colored curves are model calculations with a $D_{\mu\mu} \propto (1-\mu^2)$ (red) and a $D_{\mu\mu} \propto (1-\mu^2)|\mu|^{2/3}$ (blue) caused by the resonant scattering in the presence of Alfvénic turbulence with the Kolmogorov spectrum. The black curves are model fit with magnetic focusing with (solid) and without (dashed) constraint of nondivergence at $\mu = -1$.

.

CR distribution by inverting Equation (3).

$$\frac{f}{f_0} = I(\delta,\alpha) \int_0^{2\pi} \frac{f(\mathbf{r}((\delta,\alpha),\mathbf{p})}{f_0} d\alpha \tag{4}$$

Furthermore, if we remove the calculated contribution of CR intensity variation due to changes of particle momentum magnitude and guiding center, then we can derive the pitch angle distribution in the LISM by inverting Equation (1):

$$PAD(\mu) = \frac{f}{f_0 p^{-\gamma}} - \mathbf{G}_\perp \cdot \mathbf{R}_g \tag{5}$$

3. Result

Figure 2 shows a scattterplot of the PAD of 4 TeV CRs as a function of particle pitch-angle cosine $\mu = cos(\theta)$. We divided the plot into equal bins of pitch-angle and took the average PAD value within each bin. The result is shown by the green points with accompanying error bars in Figure 2. This makes the fitting process less biased towards the center of the scatterplot, where the data points are more densely concentrated. The pitch-angle distribution represents the particle distribution function as a function of the pitch-angle defined relative to the pristine interstellar magnetic field,

without the presence of the heliosphere at fixed energy and location. Other contributions to the production of particle flux anisotropy have been removed.

At a glance, the pitch-angle distribution appears to be a single-value function, though some data points carry sizable error bars. Normally, a two-dimensional angular sky map should have two angular coordinates. The fact that our distribution depends only on the pitch-angle confirms that the CR distribution in the interstellar reference frame is gyrotropic. In other words, the time-scale of gyration around magnetic field lines is very small compared to the time-scales of all other particle transport mechanisms, including scattering and diffusion.

The pitch-angle distribution allows us to reveal the physics of particle scattering by the interstellar magnetic field and turbulence. The distribution is almost linearly proportional to μ. According to the CR transport theory in the diffusive approximation [e.g. 11] the following relation holds:

$$f(\mu) = f_0 - \frac{v}{2}\nabla_{||} f_0 \int_0^{\mu} d\mu \frac{1-\mu^2}{D_{\mu\mu}}, \tag{6}$$

Here v is the particle speed, $\nabla_{||} f_0$ is the CR density gradient parallel to the magnetic field, and $D_{\mu\mu}$ is the pitch angle diffusion coefficient. The linear dependence indicates isotropic pitch-angle scattering with a $D_{\mu\mu} \propto (1-\mu^2)$, as shown by the blue line. If TeV CRs were resonantly scattered by an incompressible or Alfvenic interstellar magnetic field turbulence, with a Kolmogorov spectrum characterized by a power slope of $-5/3$, $D_{\mu\mu}$ would be proportional to $(1-\mu^2)|\mu|^{2/3}$, which would yield a pitch angle distribution that follows the red curve. The data obviously rule out such a scenario. We have three hypotheses to explain the nearly isotropic pitch angle scattering we observe: (1) Interstellar turbulence on the scales relevant to TeV CRs (roughly tens to thousands of AU) is dynamic and can disrupt resonance with particle gyration, (2) Interstellar turbulence is compressible rather than Alfvenic, or (3) The slope of the Kolmogorov power spectrum deviates significantly from $-5/3$ to -1 in the wavelength range resonating with these particles.

We notice that the data demonstrate a significant deviation from the linear fit at high μ. The fact that most data points in that range lie above the line suggests that particles become increasingly field-aligned towards $\mu = 1$. In other words, the data indicates focusing by an inhomogeneous large-scale magnetic field. The equation governing particle pitch diffusion with magnetic focusing is the following:

$$\frac{\partial}{\partial\mu} D_{\mu\mu} \frac{\partial f}{\partial\mu} + \frac{\partial}{\partial\mu} D_{\mu p} \frac{\partial f}{\partial p} - B_\mu \frac{\partial f}{\partial\mu} = \frac{\partial f}{\partial t} + v\mu\nabla_{||} f \tag{7}$$

Here, we have a focusing rate $B_\mu = v(1-\mu^2)/(2L_B)$ with magnetic field strength gradient $L_B^{-1} = -\nabla_{||} \ln B_{ism}$. If pitch-angle scattering is fast compared to the time and spatial variation scales on the right-hand side of Equation (7), we can use a quasilinear approximation similar to [11]. Using an isotropic pitch angle scattering, i.e., $D_{\mu\mu} = D_{\mu 0}(1-\mu^2)$ and $D_{\mu p} = D_{p0}(1-\mu^2)$ with a constant $D_{\mu 0}$ and D_{p0}, we can solve Equation (7):

$$\begin{aligned} f(\mu) = f_0 \quad &+ \quad C_1 \left\{ \exp(B_0) \left[\mathrm{ei}(-B_0 - B_0\mu) - \mathrm{ei}(-B_0) \right] \exp(-B_0) \left[\mathrm{ei}(B_0 - B_0\mu) - \mathrm{ei}(B_0) \right] \right\} \\ &- \quad \frac{1}{2B_0^2 D_0} \left(v\nabla_{||} f_0 + D_{p0} \frac{\partial f_0}{\partial p} \right) \left[(1+B_0)\ln(1+\mu) + (1-B_0)\ln(1-\mu) \right] \\ &- \quad \frac{1}{2B_0 D_0} \frac{\partial f_0}{\partial t} \left[\ln(1-\mu) + \ln(1+\mu) \right] \end{aligned} \tag{8}$$

Here, $B_0 = v/(2L_B D_0) = \lambda_{||}/L_B$, ei() is the exponential integral, and C_1 is an integration constant to be fixed by the boundary condition at the nodes $\mu = \pm 1$. We have assumed that the diffusive condition is valid, such that the terms on the right-hand side of Equation (7) are small and the derivatives $\partial f_0/\partial t$, $\nabla_{||} f_0$ and $\partial f_0/\partial p$ do not depend on μ. Normally, without the focusing term or $B_0 = 0$, C_1 can be set so that $f(\mu = \pm 1)$ is finite. However, this cannot be guaranteed in our case. The pitch angle distribution scatterplot in Figure 2 displays a trend of divergence at $\mu = 1$. We fit Equation (8) to the measured data in Figure 2. The black lines represent two different fits. The solid line is constrained, whereas the dashed line is allowed to diverge also at $\mu = -1$. Both fits are very close, and yield roughly the same parameters:

$$\frac{1}{B_0 D_0}\frac{\partial \ln f_0}{\partial t} < 0.002 \tag{9}$$

$$B_0 = \frac{\lambda_{||}}{L_B} = 0.16 \pm 0.05 \tag{10}$$

$$\lambda_{||}\nabla_{||} \ln f_0 = -0.0024 \pm 0.0004 \tag{11}$$

We have neglected the the contribution from the $\partial f_0/\partial p$ term, because $D_{p0}/(pD_{\mu 0}) \sim V_A/c$ where $V_A \approx 30$ km/s is the Alfven speed in the LISM.

4. Summary

We corrected the arrival direction of CRs by taking into account the bending of particle trajectories by the heliospheric magnetic field. The mapped CR distribution function is normalized for each latitude before being fitted to observations, thus mitigating the experimental blindness to latitudinal variations of CR flux. These procedures have allowed us to derive the true pitch angle distribution of TeV CRs in the original LISM. The resulting distribution is almost a linear function of μ, which indicates nearly isotropic pitch angle scattering by the interstellar magnetic field turbulence. We observed an excess of particle flux towards $\mu = 1$ compared to the prediction made by a linear fit. This is likely a result of focusing by an inhomogeneous interstellar magnetic field, which becomes weaker along the field line into the northern Galactic halo. The gradient length of magnetic field strength L_B is about 6 times the particle mean free path $\lambda_{||}$. The gradient scale of particle flux along the field line is about 416 times the particle mean free path.

References

[1] Abbasi, R., Abdou, Y., Abu-Zayyad, T., et al. 2011, ApJ, 740, 16-32.

[2] Amenomori, M. et al. 2006, Science, 439-443.

[3] Abeysekara, A.U., et al., 2019, ApJ, 871, 96-110.

[4] Borovikov, S. N. & Pogorelov, N.V. 2014, ApJ, 783, 16.

[5] Heerikhuisen, J. Pogorelov, N. Brand, P. 2010, AIP Conference Proceedings 1216, 543–546.

[6] Kim T. K. et al., 2016, ApJ, 832, 72.

[7] Kim, T. K. Pogorelov, N. and Burlaga, L. F. 2017, ApJL, 843, L32.

[8] McComas, D. J. et al., 2009, Science, 326, 959.

[9] Pogorelov, N. and Borovikov, S. and Heerikhuisen, J. and Zhang, M., 2015, ApJL, 812, L6-12.

[10] Pogorelov, N. and Borovikov, S. and Heerikhuisen, J. and Zhang, M., 2017, Space Sci. Rev., 212, 193-248.

[11] Schlickeiser, R. 1989, ApJ, 336, 243-293.

[12] Stone, E. C. et al., 2005, Science, 309, 2017-2020.

[13] Stone, E. C. et al., 2008, Nature, 454, 71–74.

[14] Stone, E. C. et al., 2013, Science, 341, 150-153.

[15] Singh, T. et. al, 2018, ApJ, 864, 18.

[16] Singh, T. et al., 2019, ApJL, 875, L17.

[17] Yalim, M. S. et al., 2017, J. Phys.: Conf. Ser., 837, 012015.

[18] Zhang, M. and Zuo, P. and Pogorelov, N., 2014, ApJ, 790, 5-21.

[19] Zhang, M. et. al., ApJ, 889, 96, 2020.

[20] Zirnstein, E. J. et al., 2016, A&A, 586, 13.